Advanced Speed Control of Dual Induction Motor Using Five Leg Inverter

A main project Submitted in partial fulfilment of the requirements
for the award of the degree of

BACHELOR OF TECHNOLOGY

IN

ELECTRICAL AND ELECTRONICS ENGINEERING

Submitted by

M.KIRAN KUMAR (17091A0228)

S.SAIKRISHNA(17091A0256)

S.V.SHIVA NARAYANA REDDY(17091A0237)

Under the Esteemed Guidance of

Mr. P. SAI SAMPATH KUMAR M. Tech, (Ph.D)

Assistant Professor, Dept. of E.E.E

(ESTD-1995)

DEPARTMENT OF ELECTRICAL AND ELECTRONICS ENGINEERING

RAJEEV GANDHI MEMORIAL COLLEGE OF ENGINEERING & TECHNOLOGY

(AUTONOMOUS)

(Approved by AICTE New Delhi, Accredited by NAAC-A^{+} Grade,

Accredited by NBA, Affiliated to J.N.T. University Ananthapur)

Nandyal-518501, Kurnool Dist., A.P

2017-2021

RAJEEV GANDHI MEMORIAL COLLEGE OF ENGINEERING & TECHNOLOGY
(AUTONOMOUS)

(Approved by AICTE New Delhi, Accredited by NAAC-A+ Grade,
Accredited by NBA, Affiliated to J.N.T. University Ananthapur)
Nandyal-518501, Kurnool Dist., A.P

(ESTD-1995)

DEPARTMENT OF ELECTRICAL AND ELECTRONICS ENGINEERING

CERTIFICATE

This is to certify that the thesis entitled "ADVANCED SPEED CONTROL OF DUAL INDUTION MOTOR USING FIVE LEG INVERTER" that is being submitted by), M.KIRAN KUMAR (17091A0228), S.SAI KRISHNA (17091A0256),S.V.SHIVA NARAYANA REDDY (17091A0237) have carried out the main project for the fulfilment of the award of Bachelor of Technology in Electrical and Electronics Engineering in Rajeev Gandhi Memorial college of Engineering & technology(Autonomous) and this is a record of bona fide record of the work done by them during 2020-21. The results embodied in this project work have not been submitted to any other university or institute for the award of any degree.

Head of the Department

Dr. V. Naga Bhaskar Reddy Ph.D, MISTE
Professor

Dept. of EEE, RGMCET

Project Guide

Mr .P . Sai Sampath Kumar M.Tech(Ph.D)
Assistant Professor

Dept. of EEE, RGMCET

Signature of External Examiner:

Date:

ACKNOWLEDGEMENT

We earnestly take the responsibility to acknowledge the following distinguished personalities who graciously allowed us to carry out our project work successfully.

First we express our thanks to **Mr. P. Sai Sampath Kumar** **M. Tech,(Ph.D)** Assistant Professor of the Electrical and Electronics Engineering department, as a project guide with whose skilful concomitance the excellence has been exemplified in bringing out this main project work with artistry and for the encouragement which contributed to the successful completion of the main project.

We would like to thank our electrical department for giving us permission to do the main project. At the outset we thank our honourable chairman **Dr. M. SANTHI RAMUDU garu**, for providing us with good faculty and for his moral support throughout the course.

We are perspicuous to divulge our sincere thanks to our principal, **Dr. T. JAYA CHANDRA PRASAD garu**, who has been observed posing violence in abundance forwards our individuality to our main project work tendentiously.

We manifest our capabilities and heartier thankfulness pertaining to our Head Of Department **Dr.V.Naga Bhaskar Reddy,** with whose adroit concomitance the excellence has been exemplified in bringing out this main project work with artistry.

A heart full and sincere gratitude to our beloved parents for their tremendous motivation and moral support. Finally we express our gratitude to our friends and others who have helped us directly and indirectly in carrying our project work successfully.

PROJECT ASSOCIATES

M.KIRAN KUMAR (17091A0228)

S. SAIKRISHNA (17091A0256)

S.V.SHIVA NARAYANA REDDY (17091A0237)

ABSTRACT

This paper proposes advanced speed control for a five-leg voltage source inverter (FLVSI) that drives the dual three-phase induction motor system used in industrial manufacturing processes. The advanced speed control method consists of two controllers. The first is a slip controller that satisfies the application requirement, i.e., to control the mechanical speed of two motors equally regardless of the load condition. The second is an angle controller that satisfies the FLVSI requirement, i.e., to control the phase angle difference between the two motors for minimizing the common leg current because the common leg current can be twice higher than other leg`s current depending on the operation condition of the dual-motor. And the whole performance of the advanced speed control for FLVSI fed the dual-motor drive system is shown to identify its feasibility through the experimental results.

LIST OF CONTENTS

LIST OF FIGURES

CHAPTER-1

INTRODUCTION

1.1 Introduction

High efficiency, high performance and low-cost AC motor drive systems are required in many industrial applications, induction motor drive system along with low cost and robustness is mainly used in various industrial applications. Many industrial manufacturing processes in the textile, paper, and steel industries require numerous electric machines [1]-[4].

Over the past decade, dual-motor drive systems have received considerable attention for reducing the size, number of devices, and losses of the inverters. For driving the dual-motor system different topologies of the voltage source inverter have been investigated [5]-[7], such as the mono inverter dual parallel system [8], the four-leg inverter system [9], the five- leg inverter system, and the nine-switch inverter system [10]. These topologies with a reduced number of switching devices can reduce the capital cost and the volume of the whole system. They can also provide the reduction of switching losses, which improves the efficiency of the motor drive system.

A five-leg voltage source inverter (FLVSI), which is a type of dual-motor drive system, can save two switches compared with two three-leg voltage source inverters (TLVSI). Many control methods have been proposed for the FLVSI dual-motor drive system such as the two-arm modulation (TAM) method [11],[12] the double zero sequence (DZS) method, space vector modulation (SVM) method [13], direct torque control (DTC) method [14] and hysteresis control method [15]. These control methods allow two motors to independently controlled and improve the voltage utilization factor [16]. In FLVSI for a dual-motor drive system, as shown in Figure 1.1, one phase of each motor is connected to the common leg of the FLVSI. Therefore, when the dual-motor system is driven, the peak value of the common leg current can be higher than the other legs, depending on the operating conditions [17]. In the worst case, the peak value of the common leg current can be twice higher than the other leg`s current. The peak value of each leg current is a very important factor for determining the rated condition of the switching device, such as the insulated-gate bipolar

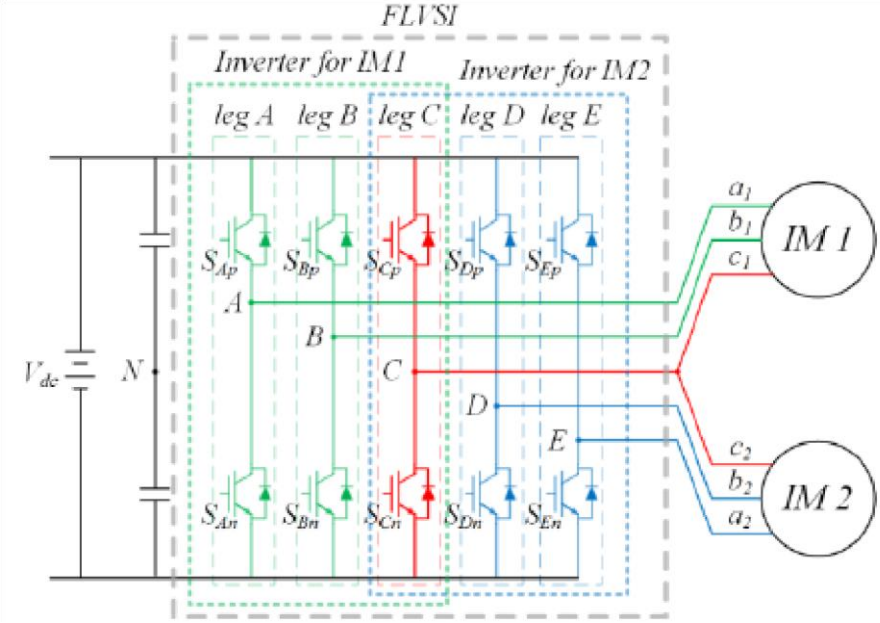

Figure 1.1: circuit configuration of the FLVSI driving a dual -motor

transistor (IGBT) that configures the FLVSI [18]. If the peak value of the common leg current is reduced, a switching device with a lower rated condition can be selected. That is, by minimizing the peak value of the common leg current, the size, weight, and capital cost of the inverter can be reduced.

In this paper, advanced speed control is proposed for the FLVSI to drive a dual induction motor system used in industrial manufacturing processes. From the application, the first requirement is suggested as the two motors should operate at the same speed regardless of the load condition of two motors. The second requirement is to minimize the common leg current derived from the applying FLVSI. In general, when the two motors are controlled independently by each general PI speed controller, depending on the phase difference between the two motors, the peak value of the common leg current can be higher than the other leg`s current. If the peak value of common leg current is controlled to the minimum regardless of the operating condition and load condition, the rated current of the switching device for the common leg can be reduced. However, the control method for minimizing the peak value of the common leg current has not been studied. This paper proposes an advanced speed control scheme that minimizes the common leg current of FLVSI controlling two motors driven at the same speed. The advanced speed control consists of two controllers. The first is an angle controller that

controls the phase angle difference between the two motors. Therefore, the two motors are controlled independently to have a constant phase angle difference; The peak value of the common leg current can be minimized. The second is a slip controller that keeps the mechanical speed of the two motors the same when the load conditions of the two motors are different? Next, the design and stability analysis for the both angle controller and the slip controller is implemented. The proposed advanced speed control method is very useful in the industrial field using a dual-motor system driven at the same speed. The validity of the whole advanced speed control is demonstrated by experiment.

1.2 Induction motor

An induction motor is an AC electric motor in which the electric current in the rotor needed to produce torque is obtained by electromagnetic induction from the magnetic field of the stator winding. An induction motor can therefore be made without electrical connections to the rotor. An induction motor's rotor can be either wound type or squirrel-cage type.

Three-phase squirrel-cage induction motors are widely used as industrial drives because they are rugged, reliable and economical. Single-phase induction motors are used extensively for smaller loads, such as household appliances like fans. Although traditionally used in fixed- speed service, induction motors are increasingly being used with variablefrequency drives (VFDs) in variable-speed service. VFDs offer especially important energy savings opportunities for existing and prospective induction motors in variable-torque centrifugal fan, pump and compressor load applications. Squirrel cage induction motors are very widely used in both fixed-speed and variable-frequency drive (VFD) applications.

1.2.1 Principle of operation

In both induction and synchronous motors, the AC power supplied to the motor's stator creates a magnetic field that rotates in synchronism with the AC oscillations. Whereas a synchronous motor's rotor turns at the same rate as the stator field, an induction motor's rotor rotates at a somewhat slower speed than the stator field. The induction motor stator's magnetic field is therefore changing or rotating relative to the rotor. This induces an opposing current in the induction motor's rotor, in effect the motor's secondary winding, when the latter is short-circuited or closed through external

impedance. The rotating magnetic flux induces currents in the windings of the rotor; in a manner similar to currents induced in a transformer's secondary winding(s).

The induced currents in the rotor windings in turn create magnetic fields in the rotor that react against the stator field. Due to Lenz's Law, the direction of the magnetic field created will be such as to oppose the change in current through the rotor windings. The cause of induced current in the rotor windings is the rotating stator magnetic field, so to oppose the change in rotor-winding currents the rotor will start to rotate in the direction of the rotating stator magnetic field. The rotor accelerates until the magnitude of induced rotor current and torque balances the applied mechanical load on the rotation of the rotor. Since rotation at synchronous speed would result in no induced rotor current, an induction motor always operates slightly slower than synchronous speed. The difference, or "slip," between actual and synchronous speed varies from about 0.5 to 5.0% for standard Design ~~B~~ torque curve induction motors [30]. the induction motor's essential character is that it is created solely by induction instead of being separately excited as in synchronous or DC machines or being self- magnetized as in permanent magnet motors.

For rotor currents to be induced the speed of the physical rotor must be lower than that of the stator's rotating magnetic field (ns); otherwise, the magnetic field would not be moving relative to the rotor conductors and no currents would be induced. As the speed of the rotor drops below synchronous speed, the rotation rate of the magnetic field in the rotor increases, inducing more current in the windings and creating more torque. The ratio between the rotation rate of the magnetic field induced in the rotor and the rotation rate of the stator's rotating field is called "slip". Under load, the speed drops and the slip increase enough to create sufficient torque to turn the load. For this reason, induction motors are sometimes referred to as "asynchronous motors". An induction motor can be used as an induction generator, or it can be unrolled to form a linear induction motor which can directly generate linear motion.

1.3 Synchronous speed

An AC motor's synchronous speed(n_s), is the rotation rate of the stator's magnetic field,

$$n_s = \frac{120f}{p}$$

Where f is the motor supply's frequency, where p is the number of magnetic poles and where n_s and f have identical units. For f in unit Hertz_and ns in RPM, the formula becomes for example, for a four-pole three-phase motor, p = 4 and ns 120f/4 = 1,500 and 1,800, RPM synchronous speed, respectively, for 50 Hz and 60 Hz supply systems.

The two figures at right and left above each illustrate a 2-pole 3-phase machine consisting of three pole-pairs with each pole set 60º apart.

1.4 Slip

Slip, s, is defined as the difference between synchronous speed and operating speed, at the same frequency, expressed in rpm, or in percentage or ratio of synchronous speed. Thus $$s = \frac{n_s - n_r}{n_s}$$

Where n_s is stator electrical speed, n_r is rotor mechanical speed. Slip, which varies from zero at synchronous speed and one when the rotor is at rest, determines the motor's torque. Since the short-circuited rotor windings have small resistance, even a small slip induces a large current in the rotor and produces significant torque. At full rated load, slip varies from more than 5% for small or special purpose motors to less than 1% for large motors. These speed variations can cause load-sharing problems when differently sized motors are mechanically connected. Various methods are available to reduce slip, VFDs often offering the best solution.

1.5 Converter

The term "Converters" is used to refer a system which transforms one form of electrical energy into another form of electrical energy. For example, AC into DC or DC into AC. Here conversion of ac into dc is called as "rectification" and conversion of dc into ac is known as "inversion". The power conversion systems can be classified according to the type of the input and output power

- AC to DC (rectifier)
- DC to AC (inverter)

1.5.1 AC to DC converters (Diode bridge rectifier)

A diode rectifier circuit converts ac input voltage into a fixed dc voltage. The input voltage may be single phase or three-phase. These circuits convert constant ac voltage to variable dc output voltage. These rectifiers use line voltage for their commutation. These are used in dc drives, chemical industries, and synchronous machines. Phase controlled converters may be fed from single phase and three- phase source.

1.5.2 DC to AC converters (inverter)

DC to AC converters produces an AC output waveform from a DC source. Applications include Flexible AC transmission systems (FACTS), voltage compensators, and photovoltaic inverters. Topologies for these converters can be separated into two distinct categories: voltage source inverters and current source inverters. Voltage source inverters (VSIs) are named so because the independently controlled output is a voltage waveform. Similarly, current source inverters (CSIs) are distinct in that the controlled AC output is a current waveform.

DC to AC power conversion is the result of power switching devices, which are commonly fully controllable semiconductor power switches. The output waveforms are therefore made up of discrete values, producing fast transitions rather than smooth ones. For some applications, even a rough approximation of the sinusoidal waveform of AC power is adequate. Where a near sinusoidal waveform is required, the switching devices are operated much faster than the desired output frequency, and the time they spend in either state is controlled so the averaged output is nearly sinusoidal. Common modulation techniques include the carrier-based technique, or Pulse-width modulation, space-vector technique, and the selective-harmonic technique.

Voltage source inverters have practical uses in both single-phase and three-phase applications. Single-phase VSIs utilize half-bridge and full-bridge configurations, and are widely used for power supplies, single-phase UPSs, and elaborate high-power topologies when used in multicell configurations. Three-phase VSIs are used in applications that require sinusoidal voltage waveforms, such as ASDs, UPSs, and some types of FACTS

devices such as the STATCOM. They are also used in applications where arbitrary voltages are required as in the case of active power filters and voltage compensators.

Current source inverters are used to produce an AC output current from a DC current supply. This type of inverter is practical for three-phase applications in which high-quality voltage waveforms are required.

A relatively new class of inverters, called multilevel inverters, has gained widespread interest. Normal operation of CSIs and VSIs can be classified as two-level inverters, due to the fact that power switches connect to either the positive or to the negative DC bus. If more than two voltage levels were available to the inverter output terminals, the AC output could better approximate a sine wave. It is for this reason that multilevel inverters, although more complex and costly, offer higher performance.

Each inverter type differs in the DC links used, and in whether or not they require freewheeling diodes. Either can be made to operate in square-wave or pulsewidth modulation (PWM) mode, depending on its intended usage. Square-wave mode offers simplicity, while PWM can be implemented several different ways and produces higher quality waveforms.

1.6 Literature Survey

H. Shin, S. Kang, and K.-B. Lee, this paper presents a torque ripple reduction method of direct torque control (DTC) using fuzzy controller with optimal selection strategy of voltage vectors in a five-phase induction motor. The conventional DTC method has some drawbacks. First, switching frequency changes according to the hysteresis bands and motor's speed.

C. S. Lim, E. Levi, M. Jones, N. A. Rahim This paper presents an investigation of the finite-control-set model predictive control (FCS-MPC) of a five-phase induction motor drive. Specifically, performance with regard to different selections of inverter switching states is investigated. The motor is operated under rotor flux orientation, and both flux/torque producing (d-q) and nonflux/torque producing (x-y) currents are included into the quadratic cost function

K. Matsuse, H. Kawai, Y. Kouno, and J. Oikawa A method of improving the stability of multiple-motor drive system has been devised that employs the averages and differences of estimated parameters for field-oriented control. The parameters of each motor (stator current,

rotor flux, and speed) are estimated using adaptive rotor flux observers to achieve sensor less control.

1.7 Existing Method

Over the past decade, dual-motor drive systems have received considerable attention for reducing the size, number of devices, and losses of the inverters. For driving the dual-motor system, different topologies of the voltage source inverter have been investigated [5]– [7], such as the mono inverter dual parallel system [8], the four-leg inverter s

1.8 Proposed Method

This paper proposes advanced speed control for a five-leg voltage source inverter (FLVSI) that drives the dual three-phase induction motor system used in industrial manufacturing processes. The advanced speed control method consists of two controllers. The first is a slip controller that satisfies the application requirement, i.e., to control the mechanical speed of two motors equally regardless of the load condition. The second is an angle controller that satisfies the FLVSI requirement, i.e., to control the phase angle difference between the two motors for minimizing the common leg current because the common leg current can be twice higher than other leg`s current

1.9 Thesis overview:

The thesis explains the implementation of "**Advanced Speed Control of Dual Induction Motor Using Five Leg Inverter".** The Organization of the thesis is explained here with:

CHAPTER 1: Presents introduction to the overall thesis and the project. In this introduction of project discuss about the induction motor, principle of operation, synchronous speed, slip, converters

CHAPTER 2: Presents the Voltage source inverter, five leg-inverter, braking of induction motor and explain clearly

CHAPTER 3: Presents the controlling circuit and working of each block of control circuit of project

CHAPTER 4: Presents the advantages and application of the project

CHAPTER 5: Presents the result, conclusion and future scope of the project and references

CHAPTER-2

VOLTAGE SOURCE INVERTER

2.1 Voltage source inverter

Voltage Source Inverters (VSI) feed the output inverter section from an approximately constant-voltage source. The desired quality of the current output waveform determines which modulation technique needs to be selected for a given application. The output of a VSI is composed of discrete values. In order to obtain a smooth current waveform, the loads need to be inductive at the select harmonic frequencies. Without some sort of inductive filtering between the source and load, a capacitive load will cause the load to receive a choppy current waveform, with large and frequent current spikes. There are three main types of VSIs:

- Single-phase half-bridge inverter
- Single-phase full-bridge inverter
- Three-phase voltage source inverter

2.1.1 Single-phase half-bridge inverter

The single-phase voltage source half-bridge inverters are meant for lower voltage applications and are commonly used in power supplies. Figure 2.1.1 shows the circuit diagram of Single-Phase half-bridge inverter.Low-order current harmonics get injected back to the source voltage by the operation of the inverter. This means that two large capacitors are needed for filtering purposes in this design. As Figure 2.1.1 illustrates, only one switch can be on at time in each leg of the inverter. If both switches in a leg were on at the same time, the DC source will be shorted out.

Inverters can use several modulation techniques to control their switching schemes. The carrier-based PWM technique compares the AC output waveform, v_c, to a carrier voltage signal, v_Δ. When v_c is greater than v_Δ, S+ is on, and when v_c is less than v_Δ, S- is on. When the AC output is at frequency f_c with its amplitude at v_c, and the triangular carrier signal is at frequency $f_\Delta$with its amplitude at v_Δ, the PWM becomes a special sinusoidal case of the carrier based PWM. This case is dubbed sinusoidal pulse-width modulation (SPWM). For this, the modulation index, or amplitude-modulation ratio, is defined as $m_a = v_c/v_\Delta$.

The normalized carrier frequency, or frequency-modulation ratio, is calculated using the equation $m_f = f_\Delta/f_c$.

If the over-modulation region, ma, exceeds one, a higher fundamental AC output voltage will be observed, but at the cost of saturation. For SPWM, the harmonics of the output waveform are at well-defined frequencies and amplitudes. This simplifies the design of the filtering components needed for the low-order current harmonic injection from the operation of the inverter. The maximum output amplitude in this mode of operation is half of the source voltage. If the maximum output amplitude, m_a, exceeds 3.24, the output waveform of the inverter becomes a square wave. As was true for PWM, both switches in a leg for square wave modulation cannot be turned on at the same time, as this would cause a short across the voltage source. The switching scheme requires that both S+ and S- be on for a half cycle of the AC output period.[4] The fundamental AC output amplitude is equal to $v_{o1} = v_{aN} = 2v_i/\pi$.Its harmonics have an amplitude of $v_{oh} = v_{o1}/h$. Therefore, the AC output voltage is not controlled by the inverter, but rather by the magnitude of the DC input voltage of the inverter.

Using selective harmonic elimination (SHE) as a modulation technique allows the switching of the inverter to selectively eliminate intrinsic harmonics. The fundamental component of the AC output voltage can also be adjusted within a desirable range. Since the AC output voltage obtained from this modulation technique has odd half and odd quarter wave symmetry, even harmonics do not exist. Any undesirable odd (N-1) intrinsic harmonics from the output waveform can be eliminated.

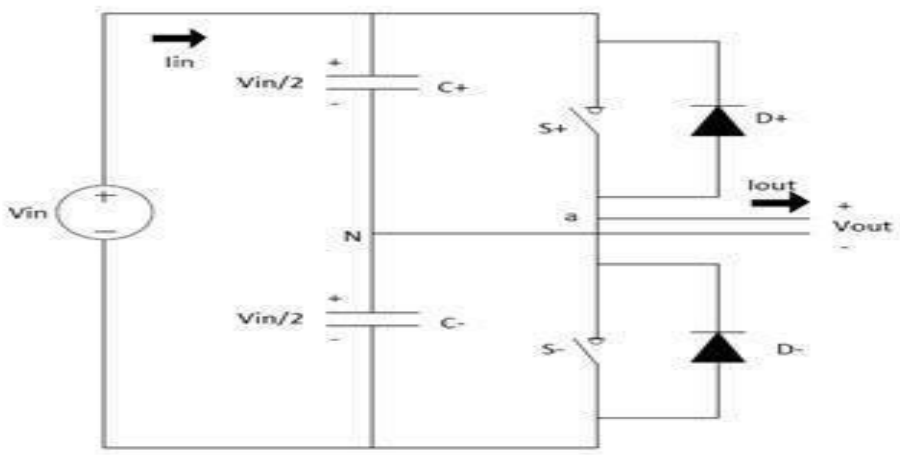

Figure 2.1.1: Single-phase Half-Bridge Voltage Source Inverter

2.1.2 Single-phase full-bridge inverter

The full-bridge inverter is similar to the half bridge-inverter, but it has an additional leg to connect the neutral point to the load. Figure 2.1.2 shows the circuit diagram of the single- phase voltage source full-bridge inverter.

To avoid shorting out the voltage source, S_{1+} and S_1- cannot be on at the same time, and S_2+ and S_2- also cannot be on at the same time. Any modulating technique used for the full- bridge configuration should have either the top or the bottom switch of each leg on at any given time. Due to the extra leg, the maximum amplitude of the output waveform is V_i, and is twice as large as the maximum achievable output amplitude for the half-bridge configuration.

States 1 and 2 are used to generate the AC output voltage with bipolar SPWM. The AC output voltage can take on only two values, either V_i or $–V_i$. To generate these same states using a half-bridge configuration, a carrier-based technique can be used. S+ being on for the half-bridge corresponds to S_1+ and S_2- being on for the full-bridge. Similarly, S- being on for the half-bridge corresponds to S_1- and S_2+ being on for the full bridge. The output voltage for this modulation technique is more or less sinusoidal, with a fundamental component that has an amplitude in the linear region of less than or equal to one $v_{o1} = v_{ab1} = v_i \cdot ma$.

Unlike the bipolar PWM technique, the unipolar approach uses states 1, 2, 3 and 4 to generate its AC output voltage. Therefore, the AC output voltage can take on the values V_i, 0 or –V [1] i. To generate these states, two sinusoidal modulating signals, Vc and –Vc, are needed, as seen in Figure 2.1.2

Vc is used to generate V_{aN}, while $–V_c$ is used to generate V_{bN}. The following relationship is called unipolar carrier-based SPWM $v_{o1} = 2 \cdot v_{aN1} = v_i \cdot m_a$.The phase voltages V_{aN} and V_{bN} are identical, but 180 degrees out of phase with each other. The output voltage is equal to the difference of the two-phase voltages, and do not contain any even harmonics. Therefore, if mf is taken, even the AC output voltage harmonics will appear at normalized odd frequencies, fh. These frequencies are centered on double the value of the normalized carrier frequency. This particular feature allows for smaller filtering components when trying to obtain a higher quality output waveform. As was the case for the half-bridge SHE, the AC output voltage contains no even harmonics due to its odd half and odd quarter wave symmetry.

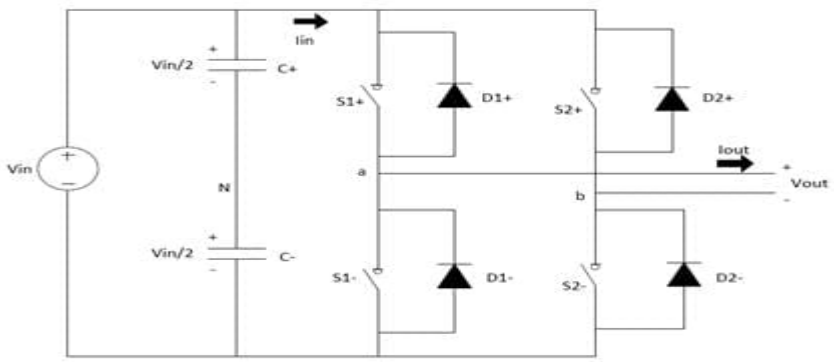

Figure 2.1.2: Single phase voltage source Full-Bridge inverter

2.1.3 Three-phase voltage source inverter

Single-phase VSI (voltage source inverter) are used primarily for low power range applications, while three phase VSIs cover both medium and high-power range applications. The circuit diagram of Three-phase VSI is shown in figure 2.1.3.

Switches in any of the three legs of the inverter cannot be switched off simultaneously due to this resulting in the voltages being dependent on the respective line current's polarity. States 7 and 8 produce zero AC line voltages, which result in AC line currents freewheeling through either the upper or the lower components. However, the line voltages for states 1 through 6 produce an AC line voltage consisting of the discrete values of V_i, 0 or $-V_i$.

For three-phase SPWM, three modulating signals that are 120 degrees out of phase with one another are used in order to produce out of phase load voltages. In order to preserve the PWM features with a single carrier signal, the normalized carrier frequency, mf, needs to be a multiple of three. This keeps the magnitude of the phase voltages identical, but out of phase with each other by 120 degrees. The maximum achievable phase voltage amplitude in the linear region, ma less than or equal to one, is $v_{phase} = v_i / 2$. The maximum achievable line voltage amplitude is $V_{ab1} = v_{ab} \cdot \sqrt{3} / 2$. The only way to control the load voltage is by changing the input DC voltage.

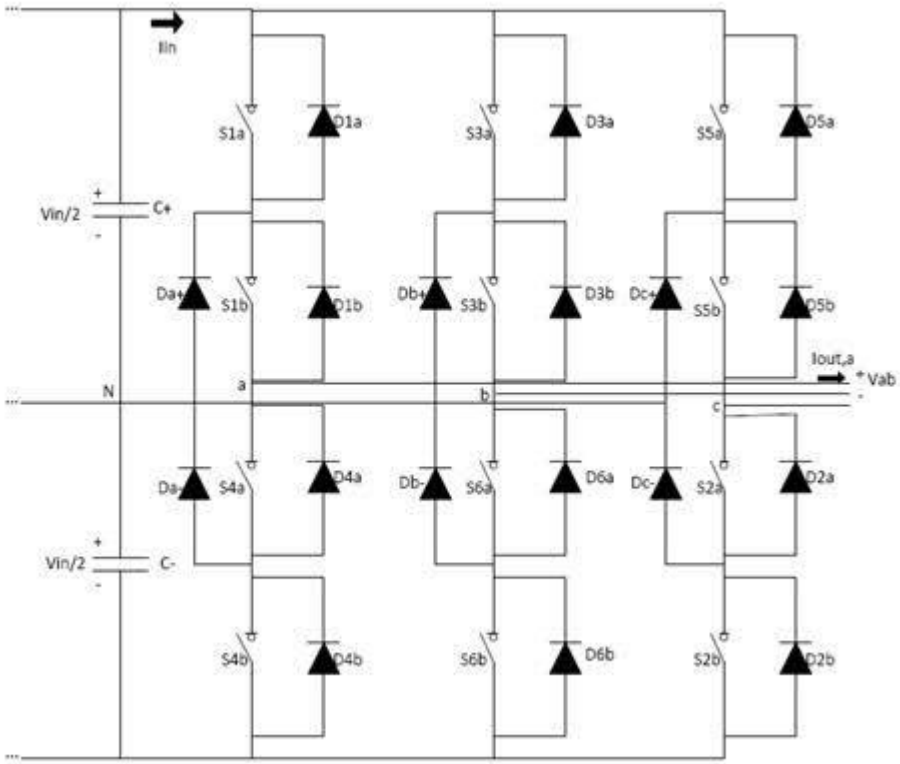

Figure 2.1.3: Three-Phase Voltage Source Inverter Circuit

2.2 Five leg-inverter

Single-phase VSIs cover low-range power applications, three-phase VSIs cover the medium to high-power applications and five-phase VSIs cover above the three-phase power applications. The main purpose of these topologies is to provide a five-phase voltage source, where the amplitude, phase, and frequency of the voltages should always be controllable. Most of the applications require sinusoidal voltage waveforms. The five-phase VSI topologies shown in figure 2.2. As in single-Leg of VSIs, the two switches (S_1 and S_6, S_3 and S_8, S_5 and S_{10}, S_7 and S_2 or S_9 and S_4) cannot be switched on at a time, because this would result in a short circuit across the dc link voltage supply. Similarly, in order to avoid undefined states in the VSI, and thus undefined ac output line voltages, the switches of any leg of the inverter cannot be switched off simultaneously as this will result in voltages that will depend upon the respective line current polarity. The circuit totally explained with six steps. During step-1, $0 \leq \omega t < \pi/5$, switches conducting 1, 8, 10, 7, 9. It is shown Figure 2.2 All impedances are same and Z_1, Z_4, Z_5 are parallel having +ve sign and Z_2, Z_3 are parallel having –ve sign. The above two combinations are in series each other.

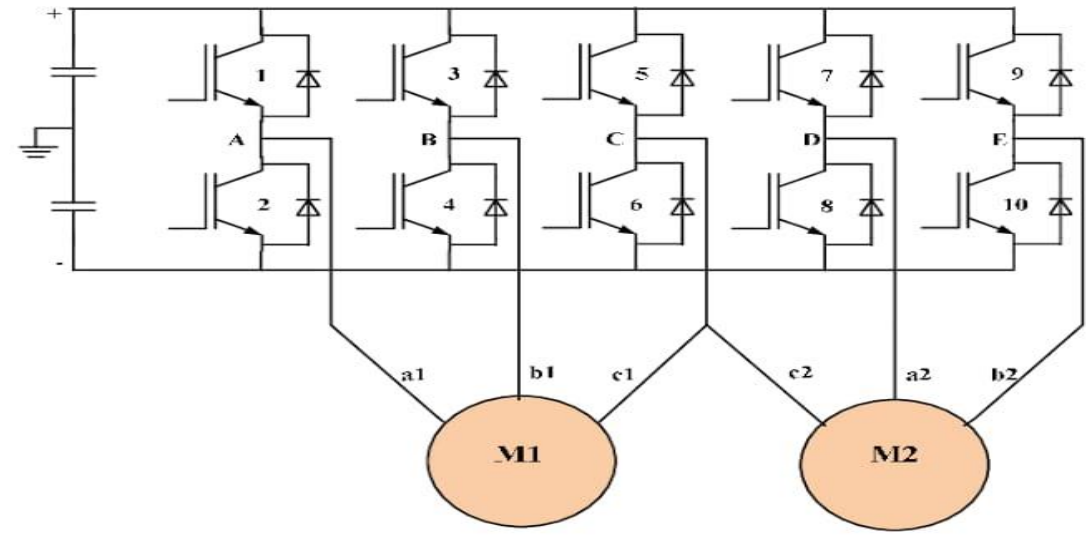

Figure 2.2: Five phase voltage source inverter topology

2.3 Braking of Induction Motors

When it comes to controlling an electric machine by electric drivers braking is a very important term because it helps to decrease the speed of the motor according to will and necessity. Braking of induction motors can be classified mainly in three types

- Regenerative braking.
- plugging or reverse voltage braking
- Dynamic braking which can be further classified as
- AC dynamic braking
- Self-excited braking using capacitors
- DC dynamic braking
- Zero sequence braking

To explain that regeneration braking for induction motor, we can take help of the equation $P_{in} = 3\ N\ I_s\ Cos\theta_s$ Here θ_s is the phase angle between the stator voltage and stator current, the simple words whenever this phase angle exceeds 90° (i.e θ_s>90°) regenerative braking can take place. To explain this more clearly and easily we can say that whenever the speed of the rotor exceeds synchronous speed, regeneration braking occurs. That is because whenever the rotor rotates at a speed more than synchronous speed there is a reverse field occurs which opposes the normal rotation of the motor and therefore braking takes place. The characteristics of regenerative braking is shown in figure 2.3.1. Main disadvantage of this type of braking is that the speed of the motor has to exceed synchronous speed which may not be possible every time. To acquire regenerative braking at a lower speed than synchronous speed, variable frequency source can be used.

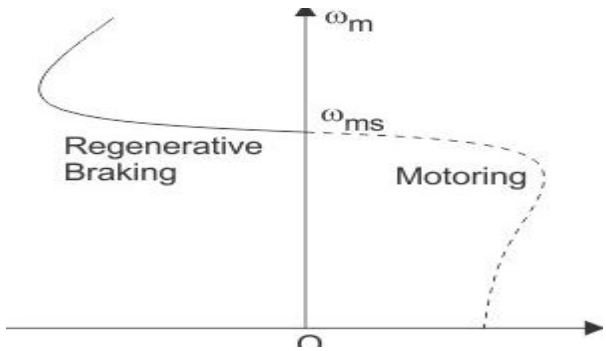

Figurer2.3.1: characteristics of regenerative breaking

Plugging of induction motors is done by interchanging any two of the supply terminals. When the terminals are reversed the operation of the machine changes from motoring to plugging as shown in figure 2.3.2. From technical point of view and for better understanding it can be said that the slip changes frm ‘s’ to (2-s), which indicates that due to reversal of the terminals the torque also changes its direction and braking occurs.

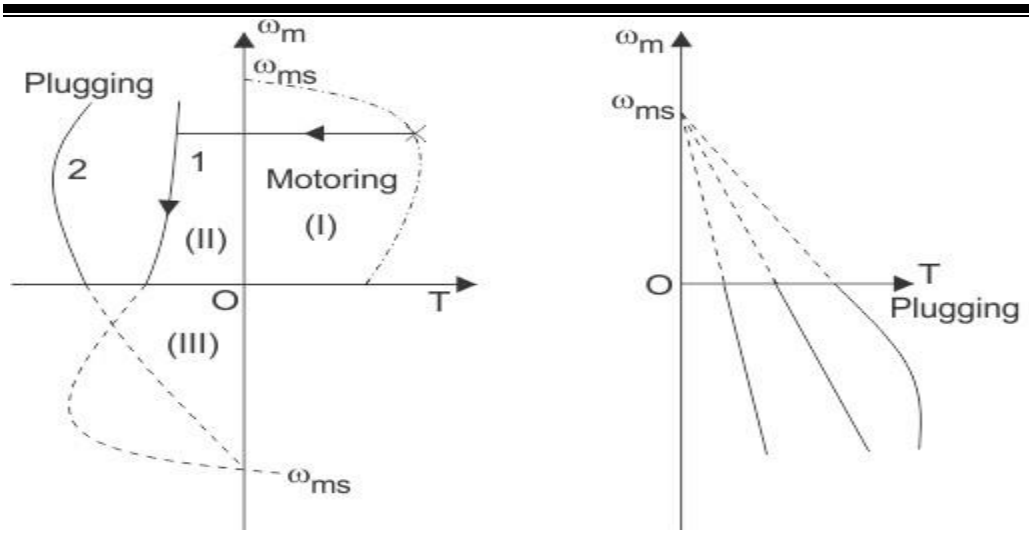

Figure2.3.2: Natural characteristics with external resistance rotor and Plugging in IV-quadrant with large external resistance in rotor

The first classification of dynamic braking of induction motors is AC dynamic breaking any one of the supply phases is disconnected from the supply and then it is either kept open or connected with the other phase. As shown in figure 2.3.3, the first type is known as two lead connection and the second one is known as three lead connection. To understand this braking method clearly, we can assume the system to be a single-phase system. Now the motor can be considered to be fed by positive and negative sequence voltages. That's why when the rotor resistance is high the net torque is negative and braking can be acquired.

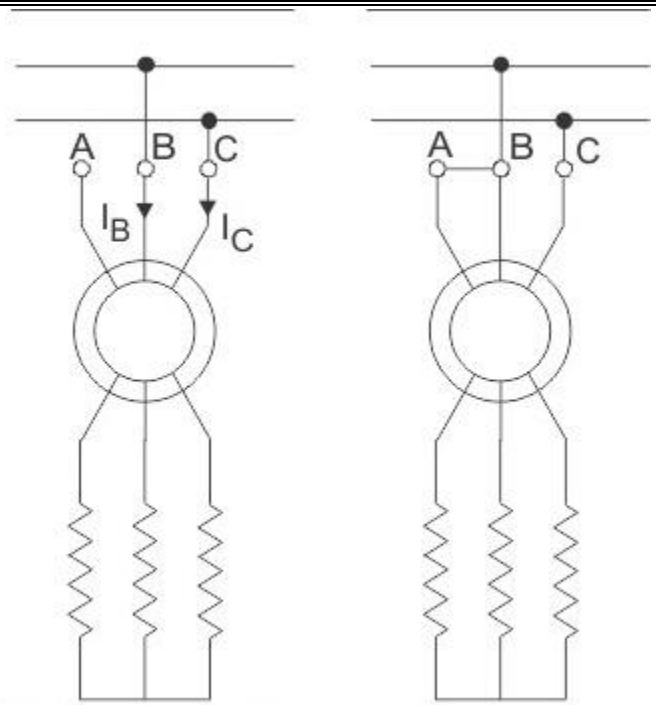

Figure 2.3.3: Two led connection and three led-connection

Sometimes capacitors are kept permanent by connected across the supply terminals of the motor. This is called self-excited braking using capacitors of induction motors. This type of braking works mainly by the property of the capacitors to store energy. Whenever the motor is disconnected from the supply the motor starts to work as a self-excited induction generator, the power comes from the capacitors connected across the terminals. The values of the capacitor are so chosen that they are sufficient to make the motor work as an induction generator after being disconnected from the supply. As shown in figure 2.3.4 when the motor works as an induction generator the produced torque opposes the normal rotation of the motor and hence braking takes place.

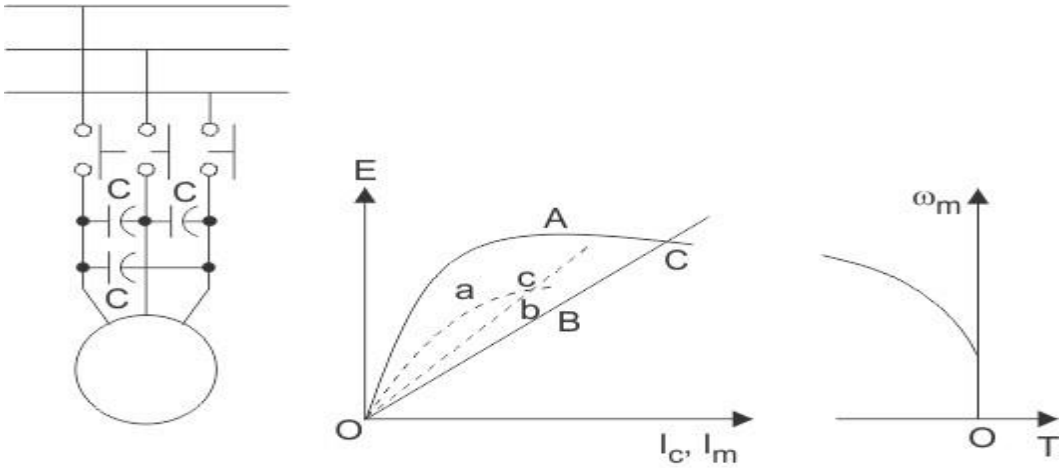

Figure 2.3.4: Characteristics of DC dynamic breaking

Another type of dynamic braking is dc dynamic braking as shown in figure 2.3.5. In this method the stator of running induction motor drives is connected to dc supply. The consequences of connecting a dc supply to the stator is as follow, the DC current produces a stationary magnetic field, in the rotor keeps rotating and as a result there is an induced voltage in the rotor winding, therefore the machine works as a generator which opposes the motion of the motor and braking is acquired

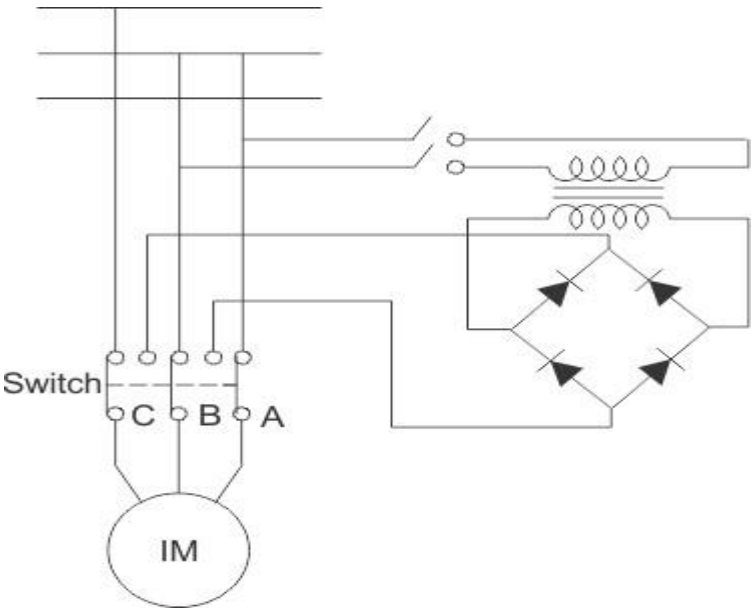

Figure 2.3.5: DC dynamic breaking

2.4 Speed Control of Induction Motors

We have discussed about the starting and braking of induction motors but what about controlling the speed during the running time. Speed control of induction motors can be done in six methods which are Pole changing

- Stator voltage control
- Supply frequency control
- Eddy –current coupling
- Rotor resistance control
- Slip power recovery

We know that the speed of the induction motor is inversely proportional to number of poles. So, it is possible to increase or decrease the speed of the induction motor if the number of the poles are decreased or increased respectively. The motor in which the provision of changing the number of poles is present, they are called 'pole changing motor' or 'multi –speed motor'. Another method of controlling the speed of induction motor drives is the stator voltage control. Stator voltage is directly responsible for the rotating speed of the rotor. Torque is proportional to voltage squared and the current is proportional to the voltage as shown in figure 2.4.1. So, if the stator voltage is reduced the speed reduces and similarly if the stator voltage is increased the speed also increases. The speed of an induction motor is proportional to the product of the supply frequency and air gap flux. But as there is a chance of magnetic saturation while decreasing the supply frequency, that's why not only the frequency but the v/f (i. e the ratio of supply voltage and frequency) is controlled and this ratio is tried to be kept constant. And if the speed is needed to be changed the ratio of v/f is changed accordingly.

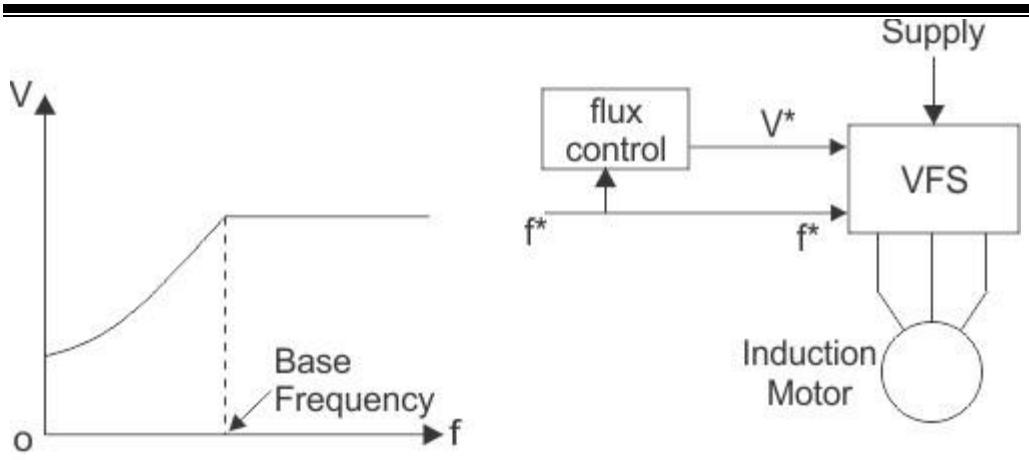

Figure2.4.1: V-f relation and variable frequency control of induction motor

The eddy current speed control method is done by placing an eddy current clutch between an induction motor is running at a fixed speed and the variable speed load .The characteristics of rotor resistance control are shown in figure 2.4.2. Now what is this eddy current clutch It is nothing but an induction motor drives in which both stator and the rotor are allowed to rotate. The rotor is coupled with the main induction motor. When eddy currents are produced in the rotor drum, their interaction with the stator field and a torque is produced which rotates the main motor. By controlling the DC current through the stator winding the speed of the motor can be controlled. Depending on the rotor resistance, the speed of the rotor falls or increases. The variation of speed torque characteristics with respect to change in rotor resistance is shown in the figure 2.4.2. This speed controlling method is better than many other methods because of low cost.

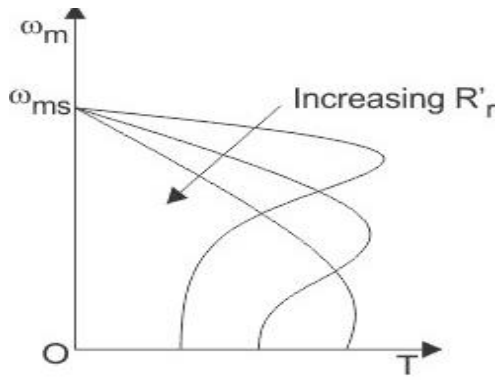

Figure 2.4.2: characteristics of rotor resistance control

2.5 Pulse width modulation:

Pulse-width modulation (PWM), or pulse-duration modulation (PDM), is a modulation technique used to encode a message into a pulsing signal. Although this modulation technique can be used to encode information for transmission, its main use is to allow the control of the power supplied to electrical devices, especially to inertial loads such as motors. In addition, PWM is one of the two principal algorithms used in photovoltaic solar battery chargers, the other being maximum power point tracking.

The average value of voltage (and current) fed to the load is controlled by turning the switch between supply and load on and off at a fast rate. The longer the switch is on compared to the off periods, the higher the total power supplied to the load.

The PWM switching frequency has to be much higher than what would affect the load (the device that uses the power), which is to say that the resultant waveform perceived by the load must be as smooth as possible. The rate (or frequency) at which the power supply must switch can vary greatly depending on load and application, for example Switching has to be done several times a minute in an electric stove; 120 Hz in a lamp dimmer; between a few kilohertz (kHz), to tens of kHz for a motor drive; and well into the tens or hundreds of kHz in audio amplifiers and computer power supplies.

The term duty cycle describes the proportion of 'on' time to the regular interval or 'period' of time; a low duty cycle corresponds to low power, because the power is off for most of the time. Duty cycle is expressed in percent, 100% being fully on.

CHAPTER- 3

CIRCUIT DESIGN AND WORKING

The configuration circuit of the FLVSI driving the two motors. It consists of a DC-source, two motors, and the FLVSI. In Figure 1.1, the two motors share the common *leg C*. Phase a_1, b_1, and c_1 of induction motor 1 (IM_1) are connected to *leg A*, *B*, and *C*, respectively. Phase a_2, b_2, and c_2 of induction motor 2 (IM_2) are connected to *leg E*, *D*, and *C*, respectively. The DC-link voltage is determined by the rated value such that the full operating range of one induction motor can be achieved.[19]-[21]

3.1 Carrier-Based PWM Strategy

The Double Zero Sequence (DZS) method of [13] is used for FLVSI driving the dual-motor system. The block diagram for the DZS method is shown in Figure3.1.1 The phase voltages for the *IM1* (*va1*, *vb1*, *vc1*), and the phase voltages for the *IM2* (*va2*, *vb2*, *vc2*) are expressed as

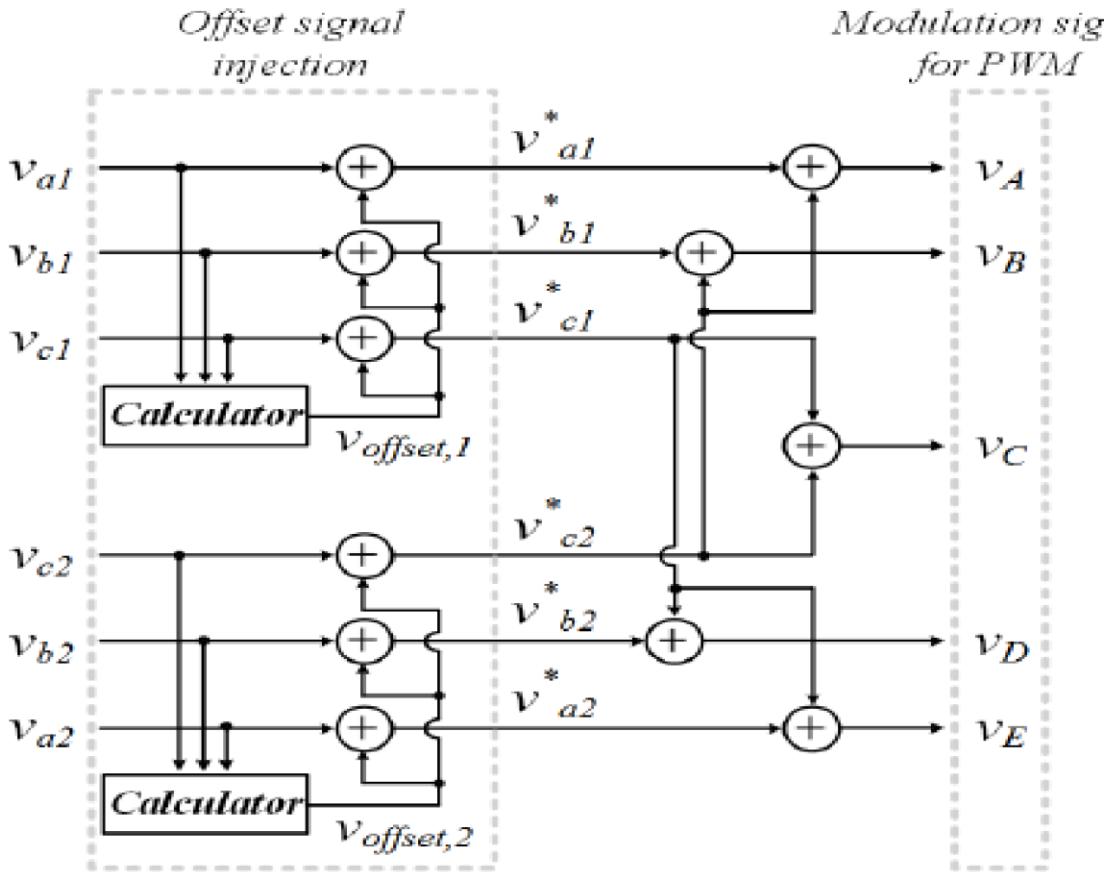

Figure3.1.1: Block diagram of Double Zero Sequence Method for the FLVSI

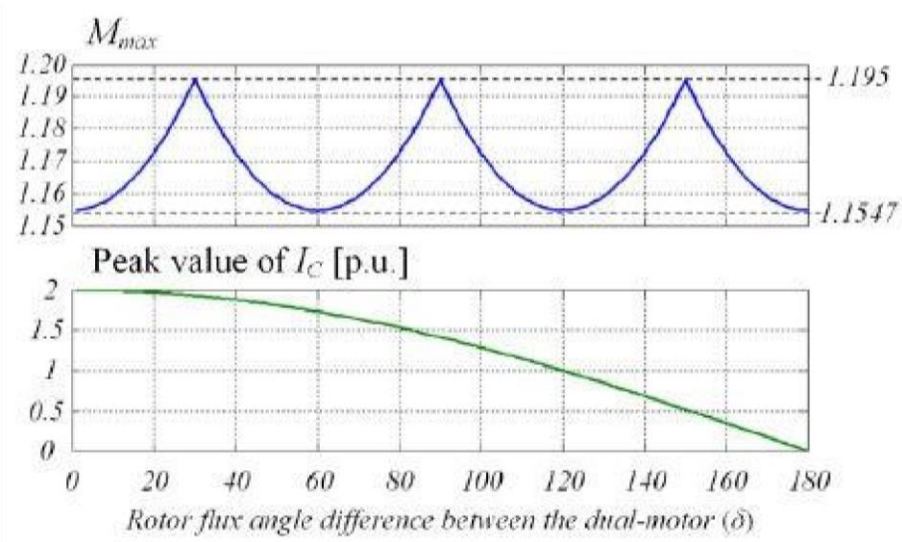

Figure 3.1.2:M_{max} and the peak value of I_c when δ changes from Zero to 180 degrees

$$\begin{aligned} v_{a1}(t) &= V_1 \sin(2\pi f_1 t + \theta_1 + \frac{2\pi}{3}), \\ v_{b1}(t) &= V_1 \sin(2\pi f_1 t + \theta_1), \\ v_{c1}(t) &= V_1 \sin(2\pi f_1 t + \theta_1 - \frac{2\pi}{3}), \end{aligned} \tag{1}$$

$$\begin{aligned} v_{a2}(t) &= V_2 \sin(2\pi f_2 t + \theta_2 + \frac{2\pi}{3}), \\ v_{b2}(t) &= V_2 \sin(2\pi f_2 t + \theta_2), \\ v_{c2}(t) &= V_2 \sin(2\pi f_2 t + \theta_2 - \frac{2\pi}{3}), \end{aligned} \tag{2}$$

where V_1 and V_2 are the phase voltage amplitude of each motor, f_1 and f_2 are the operation equency of each motor, θ_1 and θ_2 are the rotor flux angle of each motor. In the

DZS method, the offset signal (*voffset,1*, *voffset,2*) is used, which is calculated as

$$V_{offset,i} = \frac{-\{\max(V_{ai}^*, V_{bi}^*, V_{ci}^*) + \min(V_{ai}^*, V_{bi}^*, V_{ci}^*)\}}{2} \qquad (i = 1,2) \qquad (3)$$

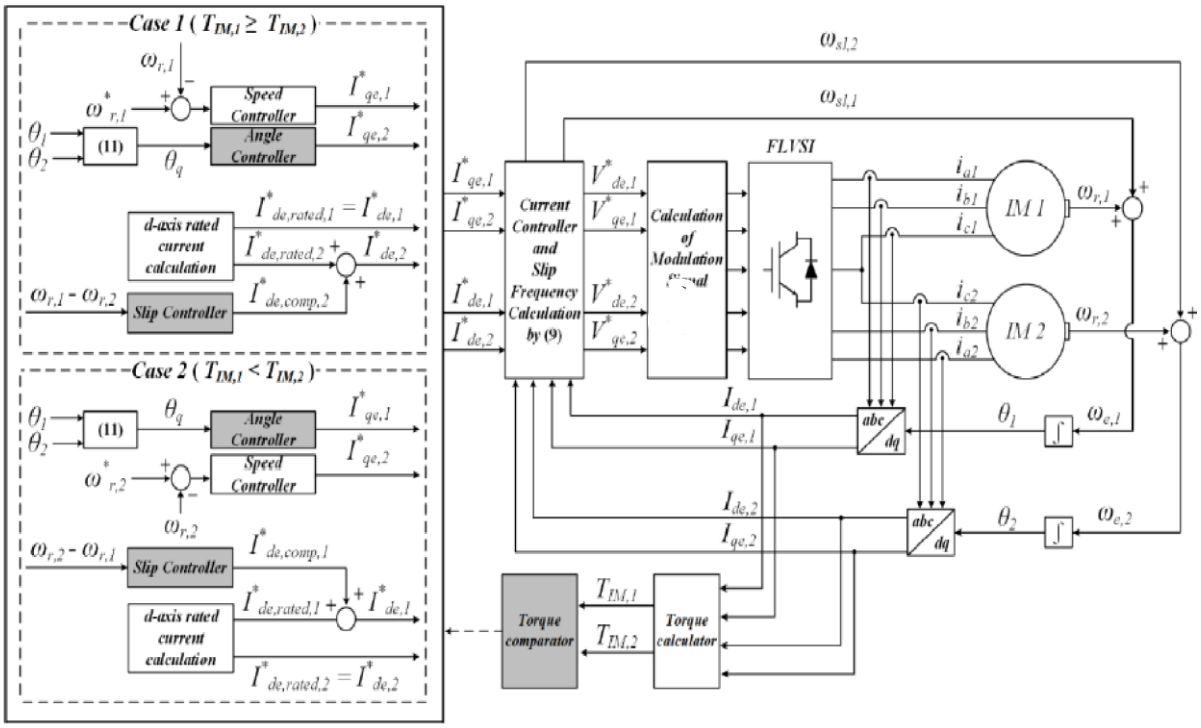

Figure 3.1.3: Control block diagram of the FLVSI system driving two induction motors

$v_{offset,1}$ and $v_{offset,2}$ is added to (v_{a1}, v_{b1}, v_{c1}) and (v_{a2}, v_{b2}, v_{c2}), respectively, as shown in Figure3.1.1. Therefore, the reference phase voltages for IM_1 (v^*_{a1}, v^*_{b1}, v^*_{c1}) and the reference phase voltages for IM_2 (v^*_{a2}, v^*_{b2}, v^*_{c2}) are calculated as

$$V^*_j = V_j + V_{offset,I} \qquad (j = a_1, b_1, c_1)$$

$$V^*_k = V_k + V_{offset,2} \qquad (k = a_2, b_2, c_2) \qquad (4)$$

From the complement signal injection of Figure 3.1.1, the modulation signals of *leg A*, *B*, *C*, *D*, and *E* (v_A, v_B, v_C, v_D, v_E) are finally generated as the sum of the reference phase voltages. The modulation index (M_1, M_2) of the two motors is defined as

$$M_1 = V_1 / 0.5V_{dc}$$

$$M_2 = V_2 / 0.5V_{dc} \qquad (5)$$

In the linear modulation region, when δ is 0, the maximum value (*Mmax*) of the sum of M_1 and M_2 is 1.1547. In the DZS method, the available *Vdc* will become automatically sub- divided between the two motors which means that the sum of M_1 and M_2 is less than

1.1547. Therefore, within the allowable range of available DC-link voltage, two motors can be controlled independently using the DZS method.

3.2. Common Leg Current

As mentioned previously, because v_A, v_B, v_C, v_D, and v_E appear as the sum of reference phase voltages, these signals may not appear in the form of a sinusoidal wave.

Additionally, the common leg current (I_C) is calculated as the sum of the phase c_1 and c_2 currents (ic_1, ic_2) and can differ from the other leg currents in form and amplitude. That is, the form and magnitude of v_A, v_B, v_C, v_D, v_E, and I_C will vary depending on the difference ($\delta = \theta_1 - \theta_2$) between the rotor flux angles of the two motors [22],[23].

Figure 3.1.2 shows the variation of M_{max} and the peak value of I_C according to the δ change under the aforementioned condition ($f_1 = f_2$, $V_1 = V_2 = V_{dc}/2$). Figure 3 shows that the allowable *Mmax*, which means that the linear modulation region varies from 1.1547 to 1.195 when δ is changed. The peak value of I_C gradually decreases as δ increases to 180 degrees. Since the linear modulation region to be extended is not large relatively, in terms of peak current, the optimal operating condition for driving two motors with FLVSI is decided as the operation when δ is 180 degrees. By considering the load conditions of the two motors in [24], the peak value of *IC* is expressed as

$$I_{C\_peak} = \sqrt{i_{c1}^2 + i_{c2}^2 + 2i_{c1}^2 i_{c2}^2 \cos(\delta)} \qquad (6)$$

According to the operating characteristics of the dual-motor system used in the application, δ and the load condition are varied. In view of reducing the rated current condition of the switching device, the best way to minimize the peak value of I_C is to keep δ constant at 180 degrees, which means that the electrical speeds of the two motors are controlled equally. Therefore, this paper proposes an advanced speed control method for the FLVSI containing the peak value minimization of I_C with the same mechanical speed regardless of the load conditions

3.3. Control Objectives

The system requirements are suggested as the two motors should operate at the same speed regardless of load conditions of the two motors *IC* should be minimized. To effectively achieve these two requirements by using the FLVSI, the advanced speed

control method contains two controllers. In the first control method which is the angle controller, δ is controlled as the constant value which is 180 degrees minimizing *Ic* regardless of the load conditions.

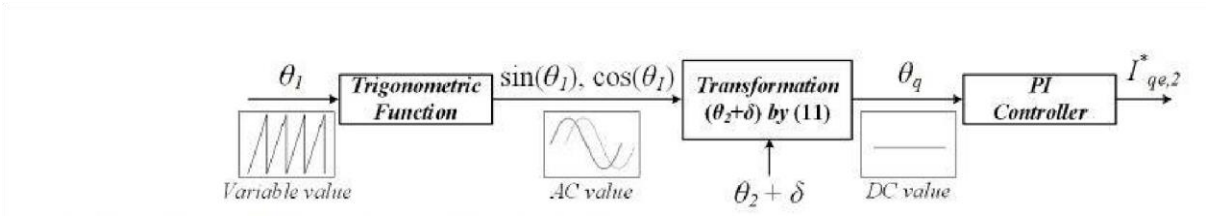

Figure 3.3.1: normalized method for the difference between the angles

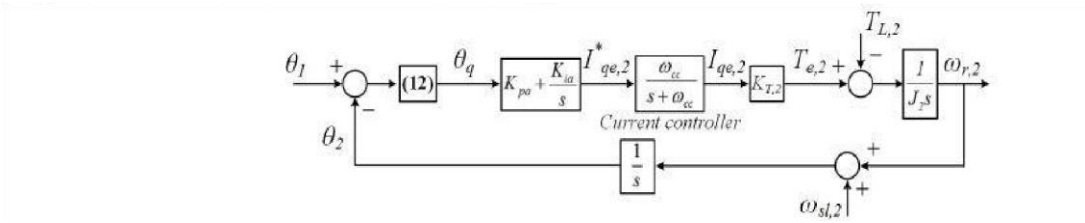

Figure3.3.2: The block diagram of the proposed angle controller

The slip controller which is the second controller is proposed to control the mechanical speed of two motors equally regardless of the load conditions.

3.4 Advanced Speed Control

Figure 3.1.3 shows the control block diagram of the FLVSI driving the two motors. To control two motors through the FLVSI, the rotor-flux-oriented vector control method of [25],[26] is implemented. Furthermore, it can be seen that FLVSI is controlled by the advanced speed control according to the load conditions of the two motors.

In the load condition of *Case 1*, where the generating torque of IM_1 is larger than the generating torque of IM_2, the *q*-axis reference current ($I^*qe,1$) for IM_1 is calculated by the output of the speed controller. The *d*-axis reference current ($I^*_{de,1} = I^*_{de,\,rated,1}$) for$IM_1$ is calculated by the rated operation condition in [27] and it is expressed as

$$I^*_{de,rated,x} = \frac{\sqrt{2} \times V_{ll,rated,x}/\sqrt{3}}{\sqrt{R_{sx}^2 + (2\pi f_{rated,x} L_{s,x})^2}} \qquad (x = 1,2) \qquad (7)$$

where $V_{ll\_rated,\,x}$ is the rated line-to-line voltage of motor, *Rs, x* is the stator resistance of the motor, $f_{rated,\,x}$ are the rated frequency of the motor and *Ls, x* is the stator inductance of the motor. On the other hand, the *q*-axis reference current ($I^*_{qe,2)}$ forIM_2 is calculated by

the output of the angle controller. The *d*-axis reference current ($I^*_{de,2}$) for IM_2 is calculated as the sum of the *d*-axis rated current ($I^*_{de,\ rated,2}$) and the compensated value ($I^*_{de,\ comp,2}$) of the output of the slip controller. In case the load condition of *Case 2*, contrary to *Case 1*, both of the proposed controllers are used to control the current for IM_1. The operation condition (*Case 1* or *Case 2*) is determined according to the torques of the two motors, as shown in Figure 4. In this paper, only *Case 1* is analysed. To control the two motors at the same speed, the synchronous angular speed ($\omega_{e,\ x}$) and slip angular speed ($\omega_{sl,\ x}$) of each motor are needed and these are expressed as

$$\omega_{e,x} = \omega_{r,x} + \omega_{sl,x} \qquad (x = 1,2) \qquad (8)$$

$$\omega_{sl,x} = \frac{R_{r,x}}{L_{r,x}} \times \frac{I^*_{qe,x}}{I^*_{de,x}} \qquad (x = 1,2) \qquad (9)$$

where *Rr, x* is the rotor resistance of the motor and *Lr, x* is the rotor inductance of the motor.

From (8), the electrical phase angle (θx) of each motor is calculated as

$$\theta_x = \int \omega_{e,x}\, dt, \qquad (x = 1,2) \qquad (10)$$

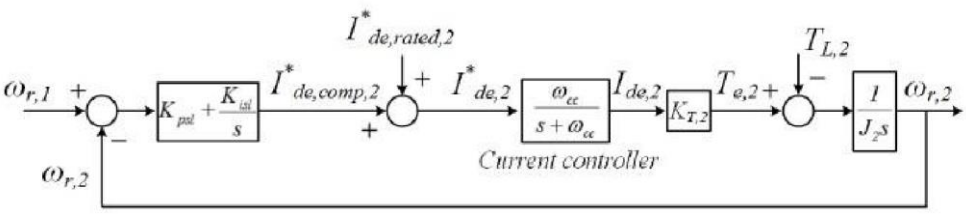

Figure3.4: The block diagram of the Proposed Slip Controller

3.5. Angle Controller

In this paper, δ is controlled as the constant value which is 180 degrees for minimizing the peak value of I_C. To maintain δ as 180 degrees, an angle controller using a general PI (proportional-integral) controller is proposed in this paper. In the angle controller, the trigonometric function is used to normalize the difference between θ_1 and $\theta_2 + \delta$ as shown in Figure 3.3.1 and its result (θq) is expressed as

$$\theta_q = -\cos(\theta_1)\sin(\theta_2 + \delta) + \sin(\theta_1)\cos(\theta_2 + \delta) \qquad (11)$$

In Figure 3.3.1, first, sin(θ_1) and cos(θ_1) appear as sinusoidal waves having a phase difference of 90 degrees with each other. Next, it can be converted into a DC value using the coordinate transformation theory in which the stationary reference frame is converted to the rotating reference frame. The θ_q calculated from θ_1 and θ_2 is used as input to the angle controller. When θ_1 and $\theta_2 + \delta$ are the same, θq is calculated as zero. That is, the normalized θq through has a physical meaning of error between θ_1 and $\theta 2 + \delta$ and the angle controller controls to be driven the two motors at the same electrical speed ($\omega e,_1 = \omega e,_2$) with the constant δ through the output $I^*qe,_2$.

Figure 3.3.2 shows the block diagram of the angle controller, where *Kpa* and *Kia* are the proportional gain and integral gain of the angle controller, respectively. ωcc is the bandwidth of the current controller, and J_2 and $KT,_2$ are the moment of inertia and the torque constant of IM_2, respectively.

3.6. Slip Controller

Through the aforementioned angle controller, IM_1 and IM_2 can be controlled at the same electrical speed ($\omega e,1 = \omega e,2$) with δ of 180 degrees. If two motors have the same parameters and the same rated condition, $I^*_{de\_rated},_1$ and $I^*_{de,\ rated},_2$ are equal. Since $\omega e,_1$ and $\omega e,_2$ is calculated by (9) and $\omega sl,_1$ and $\omega sl,_2$ have different value depending on the load conditions of the two motors, $\omega r,_1$ and $\omega r,_2$ cannot be not equal. Therefore, we propose a slip controller to operate the two motors at the same mechanical speed regardless of the load condition. The error between $\omega r,_1$ and $\omega r,_2$ becomes the input of the slip controller and the output of the slip controller is $I^*_{de,\ comp},_2$. In other words, the slip controller controls the *d* axis current of IM_2 through $I^*de,\ comp,_2$ to make the error between $\omega r,_1$ and $\omega r,_2$ zero. When the induction motor is driven, the maximum value of the *d*-axis current is limited to the rated current owing to the magnetic saturation of the

induction motor. Thus, in an FLVSI driving two motors, the slip controller compensates the *d*-axis reference current for the motor with low load conditions to regulate the slip of both motors equally.

Figure 3.4 shows the block diagram of the slip controller. *Kpsl* and *Kisl* are the proportional gain and integral gain of the slip controller, respectively. The open-loop transfer function (G_{osl}) and closed-loop transfer function (G_{csl}) are expressed as

$$G_a^o(s) = \frac{K_{psl} K_{T,2} s + K_{isl} K_{T,2}}{J_2 S^2} \quad (14)$$

$$G_{sl}^c(s) = \frac{G_{sl}^o(s)}{1+G_{sl}^o(s)} = \frac{K_{psl} K_{T,2} s + K_{isl} K_{T,2}}{J_2 s^2 + K_{psl} K_{T,2} s + K_{isl} K_{T,2}} \quad (15)$$

The configuration of the slip controller is the same as that of a general PI speed controller [29].

3.7. Analysis of the Speed Range

In FLVSI system, the available DC-link voltage is limited. Therefore, (16) is obtained by (5).

$$M_1 + M_2 \leq 1.1547 \quad (16)$$

When the proposed method is applied in FLVSI system, IM_1 and IM_2 are controlled at the same speed ($\omega e,_1 = \omega e,_2$). M_1 and M_2 are functions of *d-q* axis reference voltages ($V^*de,_1$, $V^*qe,_1$, $V^*de,_2$, $V^*qe,_2$), respectively. $V^*de,_1$, $V^*qe,_1$, $V^*de,_2$, $V^*qe,_2$ can be expressed as a function of *d-q* axis reference current ($I^*de,_1$, $I^*qe,_1$, $I^*de,_2$, $I^*qe,_2$). Therefore, the maximum speed of two motors according to the load torque variation can be calculated from the voltage limitation condition in (16) and it means the synchronous speed, which is the sum of the mechanical speed and the slip. The voltage drop due to stator resistance was neglected and the motor parameters in Table I were used during the calculation. The analysis result of speed range according to the load conditions variation when the

proposed method is applied. Under the condition of *Case 1*, it can be seen that the maximum operating speed of the two motors changes according to the load conditions.

CHAPTER -4

ADVANTAGES AND APPLICATIONS

4.1. Advantages:

By using the Five Leg Voltage Source inverter the number of switching devices are reduced which is used in Industrial Manufacturing.

Because of reducing Number of Switches switching operation is reduced and by reducing the common leg current we can use low rating switching devices which reduces the capital cost of the system

4.2. Applications:

- It is used in various Industrial applications. Such as

  1.paper manufacturing industries

  2.Text tile industries

  3. Conveyer belt industries

- High current applications. such as

  1.ship propulsion

  2.locomotive traction

  3.electrical vehicles

CHPTER-5

RESULT AND CONCLUSSION

5.1. Simulation Results

The figure 5.1.1 shows the experiment result when the two motors are controlled independently by each general PI speed controller under the load condition where the load torque for induction motor 1(T_{l1}) is 3 Nm and the load torque for IM_2(T_{L2}) is 2Nm. Since the load is same for the motors, w_{sl1}, w_{sl2} almost same and Ic value is high due to $\boldsymbol{\delta}$ is not constant

When $\delta = 0$ For Same Load and Speeds

y-axis (RPM, rad/sec, Amperes)

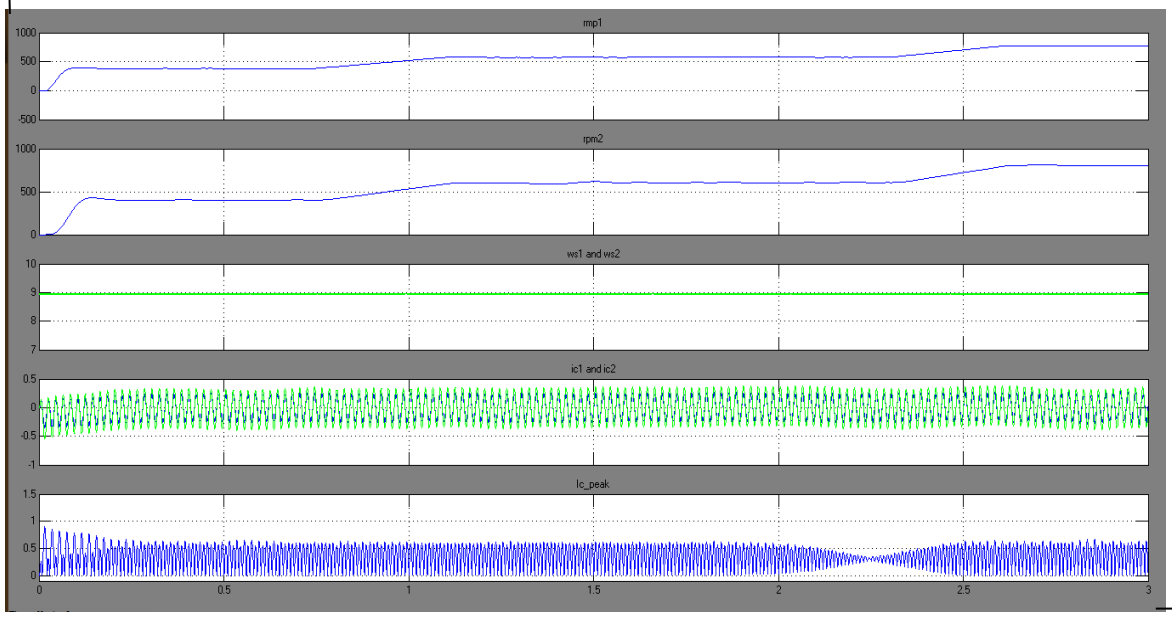

x-axis (Time(ms))

Figure 5.1.1: The same load condition (TL,1 = 3Nm, TL,2 = 3Nm) and the same speed (400rpm, 600rpm, 800rpm). ($\delta = 0$)

The figure 5.1.2 show the experiment results when the two motors are controlled by the angle controller under the load condition where T_{L1} is 3Nm and T_{L2} is 3 Nm. It is similar to above result but here through angle controller, $\boldsymbol{\delta}$ is controlled to a constant value with 180 degrees

When $\delta = 180$ For Same Speed and Load

y-axis (Rpm, rad/sec, Amperes)

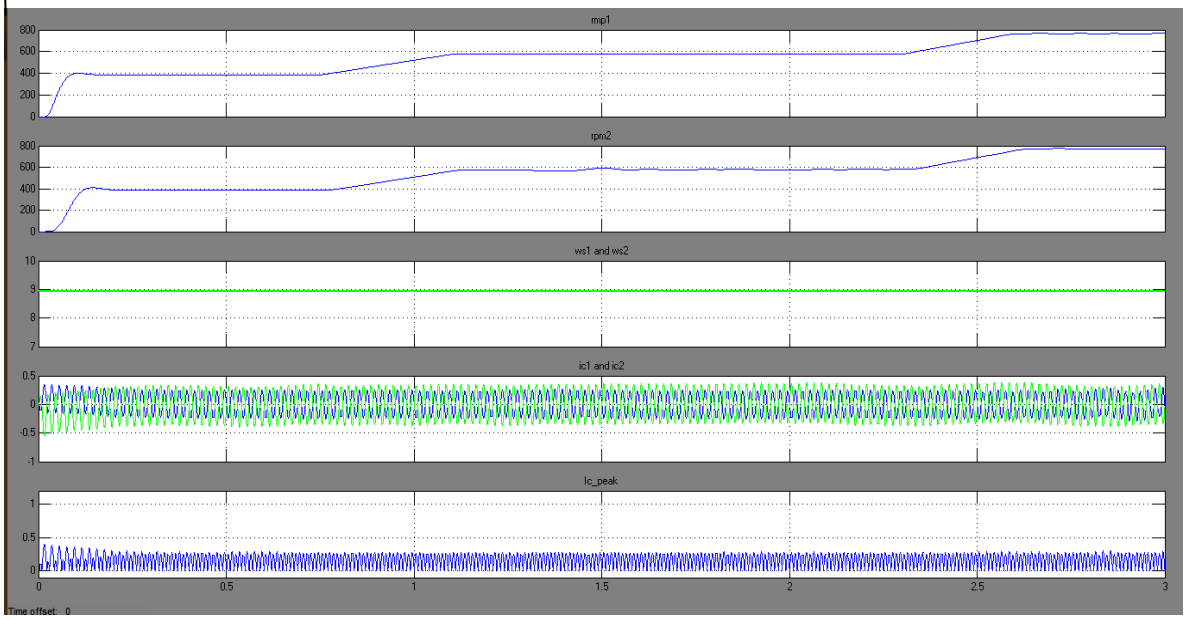

x-axis (Time(ms))

Figure 5.1.2: The same load condition (TL,1 = 3Nm, TL,2 = 3Nm) and the same speed (400rpm, 600rpm, 800rpm). ($\delta = 180$)

The figure 5.1.3 shows the experiment result when the two motors are controlled by the angle controller under the different load condition where T_{L1} is 7Nm and T_{L2} is 3Nm Here we can observe that the T_{L1} is larger than the T_{L2}, So Wsl1 is appears to be larger than Wsl2 therefore it can be seen that the mechanical speeds of the motors are different but the Ic peak value is minimized through angle controller that is $\boldsymbol{\delta}$ is maintained at constant 180 degrees

Using Angle Controller for Different Load Condition

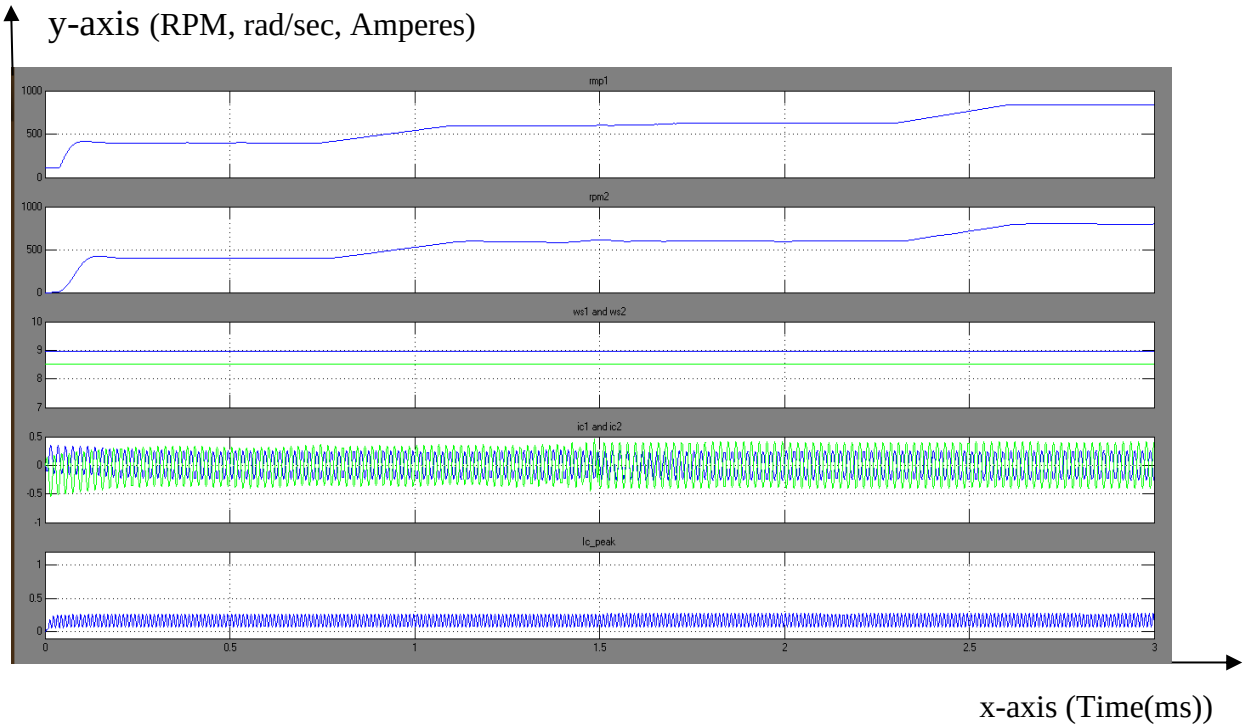

Figure 5.1.3: The different load condition (*TL,1* = 7Nm, *TL,2* = 3Nm) and the same speed (400rpm, 600rpm,800 rpm).

The figure 5.1.4 shows the experiment results when the two motors are controlled by the angle controller and the slip controller under different load condition where T_{L1} is 7Nm and T_{L2} is 3Nm. First 3 sec we can not using the angle controller and slip controller. After 3 sec we are implementing the angle controller and slip controller. by using slip controller, we set W_{sl1} and W_{sl2} equal there fore the mechanical speeds of the two motors are equal

Using Angle and Slip Controller for Different Load Conditions

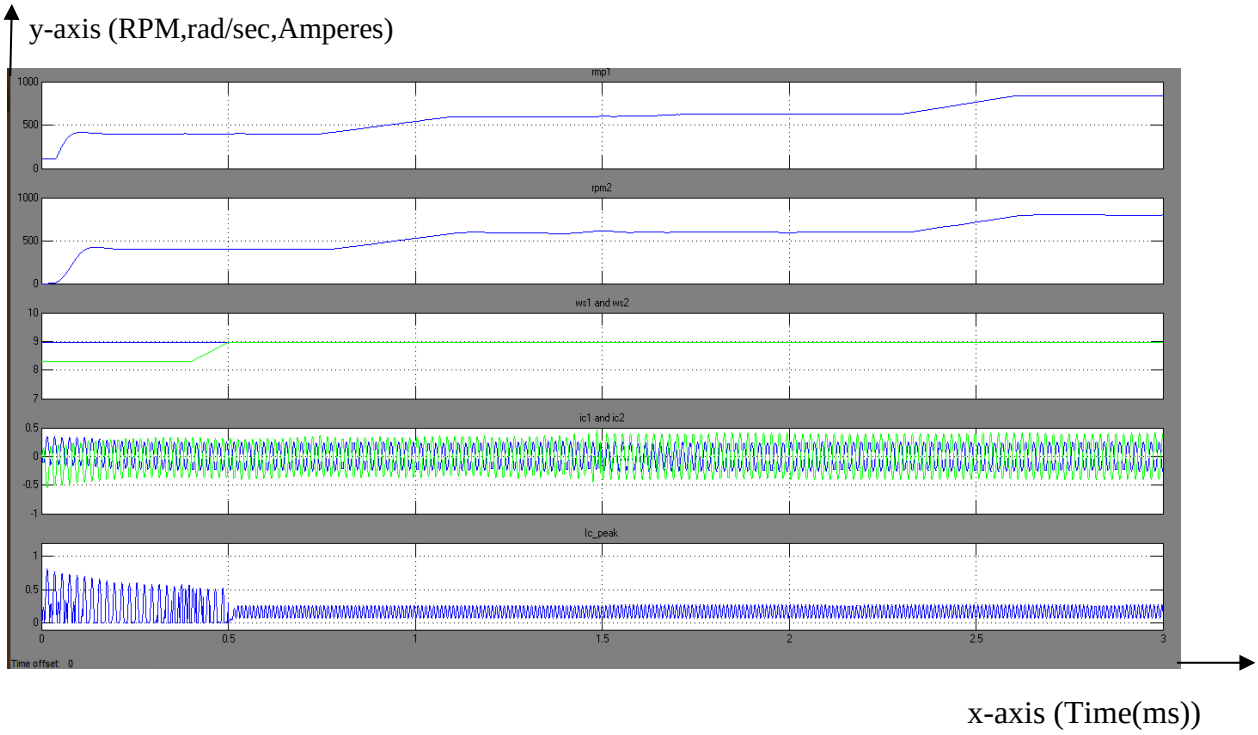

Figure 5.1.4: The simulation results when the two motors are controlled by the proposed angle controller and slip controller under the different load condition (TL,1 = 7Nm, TL,2 = 3Nm) and the same speed (400rpm ,600rpm, 800rpm).

5.2 Future Scope

This project focus on the minimizing the common leg current and maintaining the equal speed of two induction motor. It could be used in many industrial - application as paper, textile, steel industries. By using this project reduces the number of switches used in five leg-inverter to driving a dual induction motor and its better the switching operation.

Here to control the FLVSI PI controllers are used. Further development and growth can provide PID controllers. PID controllers should work better than PI because PID has three degrees of freedom (parameters that could tunes) i.e. K_p, K_i, and K_d, while PI only have two degrees of freedom i.e. K_p and K_i.

5.3 Conclusion

This paper proposed an advanced speed control method for an FLVSI that drives a dual three phase induction motor system. When using the general PI speed controller to control two motors fed by FLVSI, depending on the operating conditions of two motors, the peak value of *IC* can be higher than the other leg`s current. The proposed control method, regardless of load conditions, can minimize the peak value of *IC* of FLVSI topology, which control two motors driven at the same speed. Therefore, the proposed control scheme applied to the FLVSI can be applied to various applications (such as industrial manufacturing processes, conveyer belt) using dual induction motors. This technique consists of the two controllers (angle controller and slip controller) for satisfying two requirements: the same speed operation of the two motors and the minimization of *Ic*.. From the experimental results, the performance of the advanced speed control is proved regardless of the load conditions of the two motors.

CHAPTER-6

REFERENCES

6.1 References

1. A. Ahmed, B. -K. Koh, H. Park, K.-B. Lee, and Y. Lee, "Finite control set model redictive control method for torque control of induction motors using a state traking cost ndex," *IEEE Trans. Ind. Electron.*, vol. 64, no. 3, pp. 1916–1928, Mar. 2017.
2. H. Shin, S. Kang, and K.-B. Lee, "Torque ripple reduction in direct torque control of five-hase induction motor using fuzzy controller with optimized voltage vector selection strategy,". *Electr. Eng. Technol.*, vol. 12, no. 3, pp. 1177–1186, May 2017.
3. C. S. Lim, E. Levi, M. Jones, N. A. Rahim, and W. P. Hew, "FCS-MPC-based current control of a five-phase induction motor and its comparison with PI-PWM control," *IEEE Trans. Ind. Electron.*, vol. 61, no. 1, pp. 149–163, Jan. 2014.
4. S. Kang, H. Shin, S.-M Park, and K.-B. Lee, "Optimal voltage vector selection method for torque ripple reduction in direct torque control of a five-phase induction motor," *J. Power Electron.*, vol. 17, no. 5, pp. 1203–1210, Sep. 2017.
5. S. Tseng, T. Liu, J. Hsu, L. R. Ramelan, and E. Firmansyah, "Implementation of online aximum efficiency tracking control for a dual-motor drive system," *IET Electr. Power Appl.*, vol. 9, no. 7, pp. 449–458, Jul. 2015.
6. M. Hu, J. Zeng, S. Xu, C. Fu, and D. Qin, "Efficiency study of a dual-motor coupling EV owertrain," *IEEE Trans. Veh. Technol.*, vol. 4, no. 6, pp. 2252–2260, Jun. 2015.
7. K. Matsuse, H. Kawai, Y. Kouno, and J. Oikawa, "Characteristics of speed sensorless vector controlled dual induction motor drive connected in parallel fed by a single inverter, *IEEE Trans. Ind. Appl.*, vol. 40, no. 1, pp. 153–161, Jan./Feb. 2004.
8. Y. Lee and J.-I. Ha, "Control method of mono inverter dual parallel drive system with interior permanent magnet synchronous machines," *IEEE Trans. Power Electron.*, vol. 31, no. 10, pp. 7077–7086, Oct. 2016.
9. K. Matsuse, N. Kezuka, and K. Oka, "Characteristics of independent two induction motor drives fed by a four-leg inverter," *IEEE Trans. Ind. Appl.*, vol. 47, no. 5, pp. 2125–2134, ep. /Oct. 2011.
10. K. Oka, Y. Nozawa, R. Omata, K. Suzuki, A. Furuya, and K. Matsuse, "Characteristic omparison between five-leg inverter and nine-switch inverter," in *Proc. IEEE Power Convers. Conf.*, Jun. 2007, pp. 279–283

11. D. Dujić, M. Jones, S. Vukosavic, and E. Levi, "A general PWM method for a (2*n*+1)-e.g., inverter supplying *n* three-phase machines," *IEEE Trans. Ind. Electron.*, vol. 56, no. 10, pp. 4107–4118, Oct. 2009.
12. M. Talib, Z. Ibrahim, N. Rahim, and A. Hasim, "Implementation of space vector two arm modulation for independent motor control drive fed by a five-leg inverter," *J. Power Electron.*, vol. 14, no. 1, pp. 115–124, Jan. 2014.
13. M. Jones, S. N. Vukosavic, D. Dujić, E. Levi, and P. Wright, "Five-leg inverter PWM technique for reduced switch count two-motor constant power applications," *IET Elect Power Appl.*, vol. 2, no. 5, pp. 275–287, Sep. 2008.
14. W. Wang, J. Zhang, M. Cheng, and R. Cao, "Direct torque control of five-leg dual-MSM drive systems for fault-tolerant purposes," *J. Power Electron.*, vol. 17, no. 1, pp. 161– 1, Jan. 2017.
15. W. Wang, J. Zhang and M. Cheng, "A dual-level hysteresis current control for one five-leg VSI to control two PMSMs," *IEEE Trans. Power Electron.*, vol. 32, no. 1, pp. 804-814, Jan. 2017.
16. M. Talib, Z. Ibrahim, N. Rahim, and A. Hasim, "Analysis on speed characteristics of five leg inverter for different carrier based PWM scheme," in *Proc. IEEE Int. Power Engineering Optimization Conference (PEOCO)*, Jun. 2012, pp. 96–101.
17. M. Talib, Z. Ibrahim, N. Rahim, and A. Hasim, "Characteristic of induction motor drives fed by three leg and five leg inverters,"" *J. Power Electron.*, vol. 13, no. 5, pp. 806–813, Sep. 2013.
18. J. S. Lee and K.-B. Lee, "An open-switch fault detection method and tolerance controls based on SVM in a grid-connected T-type rectifier with unity power factor," *IEEE Trans. Ind. Electron.*, vol. 61, no. 12, pp. 7092–7104, Dec. 2014.
19. C. S. Lim, N. Abd Rahim, W. P. Hew, and E. Levi, "Model predictive control of a two-motor drive with five-leg-inverter supply," *IEEE Trans. Ind. Electron.*, vol. 60, no. 1, pp. 54–65, Jan. 2013.
20. W. Wang, M. Cheng, B. Zhang, Y. Zhu, and S. Ding, "A fault-tolerant permanent-magnet traction module for subway applications," *IEEE Trans. Power Electron.*, vol. 29, no. 4, pp. 1646–1658, Apr. 2014.
21. C. S. Lim, E. Levi, M. Jones, N. Abd. Rahim, and W. P. Hew, "A falut-tolerant two-motor drive with FCS_MP based flux and torque control," *IEEE Trans. Ind. Electron.*, vol. 61, no. 12, pp. 6603–6614, Dec. 2014.

22. [22] G. J. Su and J. S. Hsu, "A five-leg inverter for driving a traction motor and a compressor motor," *IEEE Trans. Power Electron.*, vol. 21, no. 3, pp. 687–692, May 2006.
23. C. B. Jacobina, O. I. Da Silva, E. C Santos, Jr., E. C. A. M. N. Lima, and I. S. De Freitas, "AC drive systems using five-leg converter and series-connected machines," in Proc. 2005 Power Electron. Spec. Conf. *(PESC)*, Aug. 2005, pp. 2429–2435.
24. Y. Suzuki, K. Matsuse, and H. Kubota, "Improved independed vector control of 2PMSM fed by a five-leg inverter reducing common leg peak current," in Proc. Power Electron. Appl. Conf. (PEAC*)*, Nov. 2014, pp. 527–531.
25. D. W. Novotny and T. A. Lipo, Vector Control and Dynamics of AC Drives. U. K.: Oxford Science, 1996, ch. 9.
26. A. Abdelsalam, M. Masoud, M. Hamad, and B. Williams, "Modified indirect vector control technique for current source induction motor drive," IEEE Trans. Ind. Appl., vol 48, no. 6, pp. 2433–2442, Nov. 2012.
27. M. Huang and C. Liaw, "Transient performance improvement control for ifo induction drive in field weakening region," in motor IEE Proc. Electr. Power Appl., vol. 150, no. 5, Sep. 2003, pp. 521–530.
28. K.-B. Lee, and J. S. Lee, Reliablity Improvement Technology for Power Converters. S.G.: Springer, 2017.
29. J. W. Choi and S. C. Lee, "Antiwindup strategy for PI-type speed controller," IEEE Trans. Ind. Electron., vol. 56, no. 6, pp.2039–2046, Jun. 2009.
30. Y. Wu, R. A. Mcmahon, Y. Zhan, and A. M. Knight, "Impact of PWM schemes on induction motor losses," in Conf. Rec. 41st IEEE IAS Annu. Meeting, Tampa, FL, Oct. 2006, vol. 2, p. 813–818.